PERGAMON

International Journal of Solids and Structures 36 (1999) 4725–4742

INTERNATIONAL JOURNAL OF SOLIDS and STRUCTURES

Dynamic point sources in laminated media via the thin-layer method

E. Kausel

Department of Civil Engineering, Massachusetts Institute of Technology, Cambridge, MA 02139, U.S.A.

Received 21 August 1997; accepted 20 March 1998

Abstract

This paper presents closed-form expressions for the Green's functions associated with harmonic point sources acting within horizontally layered media. These expressions are intended for use with the highly efficient Thin-Layer Method (TLM) described elsewhere, which is now being used widely for diverse engineering purposes. Among the dynamic sources considered are point forces, force dipoles (cracks and moments), blast loads, seismic double couples with no net resultant, and bimoments (moment dipoles). Comparisons with known analytical solutions for homogenous media demonstrate the accuracy of the formulation. However, the main field of application is laminated media, for which no analytical solutions can be obtained. On the other hand, it should be noted that the computational effort in this method does not depend on whether the system is layered. The resulting Green's functions could be used to efficiently model elastic waves in complex media by means of the Boundary Integral Method.

Keywords: Green's functions; Fundamental solution; Layered media; Stokes' problem; Elastodynamics; Geophysics; Boundary elements

1. Introduction

The purpose of this paper is to present the Green's functions for a class of dynamic point sources acting on, or within, laminated media. This objective is achieved using the Thin Layer Method (TLM), which is a powerful tool for the dynamic (or static) analysis of mechanical systems whose material properties change in only one coordinate direction. The set of point sources considered herein includes force dipoles (cracks, point moments, single and double couples), blast loads and bimoments (moment dipoles).

The origins of the TLM date back to the late sixties and early seventies, as detailed later. Since then, this semi-analytic method has found wide-ranging applications, such as in seismic simulation, in wave propagation through layered soils, in vibrations of laminated (or thick) plates, in soil-structure and fluid-structure interactions, in structural acoustics (diffraction and scattering problems), or in the non-destructive testing of pavements.

In essence, the method consists in a partial discretization of the wave equation, namely one in

0020-7683/99/$ - see front matter
PII: S0020-7683(98)00262-5

the direction of layering. Hence, a finite element solution is used for that coordinate direction, while closed-form solutions (or other numerical approaches) are used for the remaining coordinate directions.

2. Historical background

The TLM was first used by Lysmer (1970) to study the propagation of seismic Rayleigh waves in layered earth strata; he also formulated an equation based on Rayleigh's quotient to obtain the group velocities and the dispersion characteristics of waves as a direct by-product of the calculation and he observed that some modes may have negative group velocity. Two years later, Waas (1972) developed a very substantial extension to Lysmer's method and obtained the characteristic equations directly from a variational formulation and not from a limiting process to a finite element mesh, as Lysmer had done. He applied the method extensively to problems in two dimensions (SV-P and SH waves) and for torsional waves. Moreover, he developed a very efficient algorithm for extracting the normal modes, studied in detail the characteristics of waves in a homogeneous stratum and applied the method to obtain super-accurate transmitting boundaries for finite element representations of irregular two-dimensional soil media. These so-called consistent boundaries are equivalent to a virtual continuation of the finite element mesh to infinity; they have been implemented in well-known computer codes such as FLUSH.

Concurrently with Lysmer and Waas, the method was also independently being used by Nelson et al. (1971) and by Dong and Nelson (1972), who carried out pioneering applications of the TLM to the vibrations of laminated orthotropic cylinders and plates. At about the same time, Srinivas (1973) did analyses of composite laminates using a closely related method. In the years immediately following, the TLM was applied to the formulation of transmitting boundaries in cylindrical coordinates (Kausel, 1974); to the analysis of laminated plates and soils of finite and infinite dimensions (Kausel and Roësset, 1977); and to study the dynamic behavior of circular and annular foundations (Tassoulas, 1981).

Perhaps the most fundamental advance to the TLM came in the early eighties, when Tajimi (1980), Waas (1980) and Kausel (1981) independently applied the method to obtain the Green's functions for point forces acting on (or within) a layered medium. Of these three, the most well known came to be the latter, since it provided the most general framework for handling loads with arbitrary spatial-temporal characteristics via Fourier and Hankel transforms and included detailed expressions for the consistent strains and stresses. Based on this work, Kausel and Peek (1982a) presented the Green's functions for point forces which now lie at the heart of numerous programs and procedures for the analysis of wave motion in layered media (e.g. PUNCH, SASSI, SASW); they also applied these functions in the context of a boundary integral formulation to study laminates with irregularities, such as cavities or inclusions (Kausel and Peek, 1982b). These Green's functions were later extended to allow the modeling of layered media over elastic halfspaces (Seale, 1985; Kausel and Seale, 1987; Seale and Kausel, 1989).

More recently, the TLM was extended to study the propagation of waves in fluids (Lofti et al., 1987; Tan, 1989; Tsai et al., 1990); to assess the seismic response of earth dams (Bougacha and Tassoulas, 1991); to evaluate the response of coupled solid–fluid systems (Ghibril, 1992); and to study problems of wave propagation in poroelastic media (Bougacha et al., 1993). In the last few

years, the algorithm was reformulated and extended to laterally inhomogeneous media by Geller and Ohminato (1994), Geller and Hatori (1995), who called it the DSM method.

3. Green's functions for point forces

Consider a horizontally layered, laterally homogeneous, elastic medium described in cylindrical coordinates r, θ, z, with associated unit base vectors $\hat{\mathbf{r}}$, $\hat{\mathbf{t}}$, $\hat{\mathbf{k}}$. The material properties change only with depth. The medium consists of N layers and it is acted upon by a harmonic load at some arbitrary elevation z'.

Let u, v, w = displacement components at elevation z for a horizontal point load acting at elevation z' and U, W = displacement components for a vertical point load at these same elevations. From Kausel and Peek (1982a), the Green's functions for these loads are:

(a) Horizontal point load

$$\bar{\mathbf{g}}_x(r,\theta,z) = u\cos\theta\hat{\mathbf{r}} - v\sin\theta\hat{\mathbf{t}} + w\cos\theta\hat{\mathbf{k}} \tag{1}$$

$$u = \frac{1}{4i}\left\{\sum_{l=1}^{2N}\phi_x^l(z)\phi_x^l(z')\frac{\mathrm{d}\,H_1^{(2)}(k_l r)}{\mathrm{d}(k_l r)} + \sum_{l=1}^{N}\phi_y^l(z)\phi_y^l(z')\frac{H_1^{(2)}(k_l r)}{k_l r}\right\} \tag{2a}$$

$$v = \frac{1}{4i}\left\{\sum_{l=1}^{2N}\phi_x^l(z)\phi_x^l(z')\frac{H_1^{(2)}(k_l r)}{k_l r} + \sum_{l=1}^{N}\phi_y^l(z)\phi_y^l(z')\frac{\mathrm{d}H_1^{(2)}(k_l r)}{\mathrm{d}(k_l r)}\right\} \tag{2b}$$

$$w = -\frac{1}{4i}\sum_{l=1}^{2N}\phi_z^l(z)\phi_x^l(z')H_1^{(2)}(k_l r) \tag{2c}$$

in which ϕ_x^l, ϕ_z^l are the horizontal and vertical components of the lth SV-P ('Rayleigh') mode and ϕ_y^l are the components of the lth SH ('Love') mode. Each of these normal modes of wave propagation is associated with a (generally complex) wavenumber (eigenvalue) k_l. Also, the $H_j^{(2)}(kr)$ are second Hankel functions of order j. Notice that the Green's functions are known explicitly in the spatial domain.

(b) Vertical point load:

$$\bar{\mathbf{g}}_z(r,z) = U\hat{\mathbf{r}} + W\hat{\mathbf{k}} \tag{3}$$

$$U = \frac{1}{4i}\sum_{l=1}^{2N}\phi_x^l(z)\phi_z^l(z')H_1^{(2)}(k_l r) \tag{4a}$$

$$W = \frac{1}{4i}\sum_{l=1}^{2N}\phi_z^l(z)\phi_z^l(z')H_0^{(2)}(k_l r) \tag{4b}$$

These expressions will be used as building blocks to obtain the Green's functions for dipoles, blast loads and bimoments.

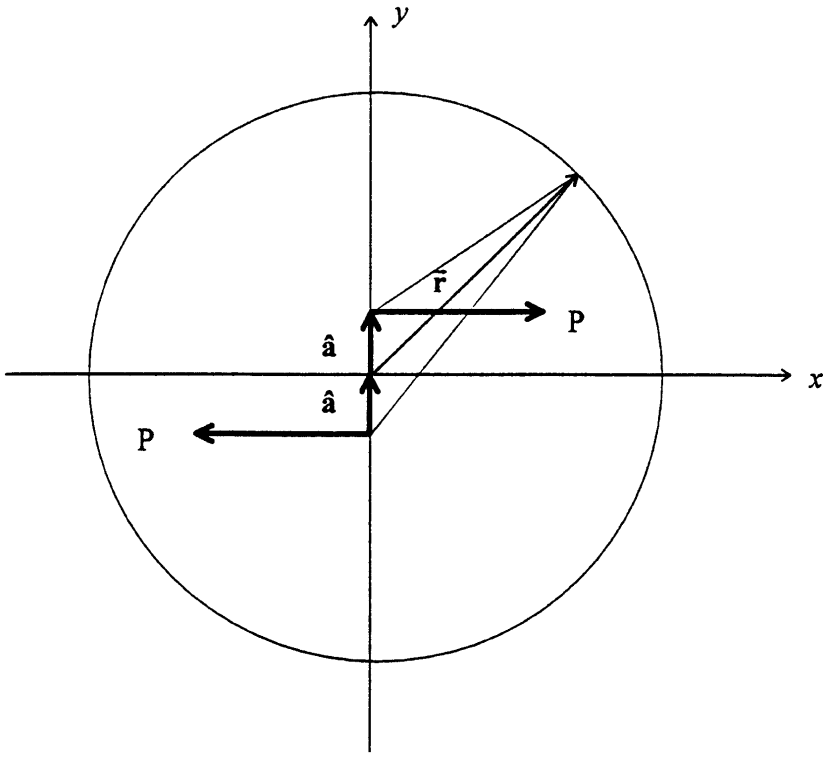

Fig. 1. Force dipole.

4. Force dipoles

Let $\bar{\mathbf{g}}(\bar{\mathbf{r}})$ be the Green's function for a point load P in some direction (say, horizontal) and apply two such loads in opposite directions at some small distance $2a$ apart (Fig. 1). Define $\bar{\mathbf{a}} = a\hat{\mathbf{a}}$ to be a vector perpendicular to these forces, of magnitude equal to their half-distance a. These forces cause a displacement field

$$\bar{\mathbf{u}} = P[\bar{\mathbf{g}}(\bar{\mathbf{r}}-\bar{\mathbf{a}}) - \bar{\mathbf{g}}(\bar{\mathbf{r}}+\bar{\mathbf{a}})] \tag{5}$$

Expand next the Green's functions in Taylor series:

$$\begin{aligned}\bar{\mathbf{g}}(\bar{\mathbf{r}}\pm\bar{\mathbf{a}}) &= \bar{\mathbf{g}}(x\pm\Delta x, y\pm\Delta y, z\pm\Delta z)\\ &= \bar{\mathbf{g}}(x,y,z)\pm\left[\frac{\partial\bar{\mathbf{g}}}{\partial x}\Delta x+\frac{\partial\bar{\mathbf{g}}}{\partial y}\Delta y+\frac{\partial\bar{\mathbf{g}}}{\partial z}\Delta z\right]+\cdots\\ &= \bar{\mathbf{g}}(\bar{\mathbf{r}})\pm\bar{\mathbf{a}}\cdot\nabla\bar{\mathbf{g}}+O(a^2)\end{aligned} \tag{6}$$

Combining eqns (5) and (6) and defining the strength M of the dipole to be $M = 2Pa$, one obtains in the limit $a \to 0$ the Green's function for a simple point dipole as

$$\bar{\mathbf{u}} = -M\hat{\mathbf{a}}\cdot\nabla\bar{\mathbf{g}} \tag{7}$$

In general, if the Green's function is expressed in cylindrical coordinates as

$$\bar{\mathbf{g}} = u\begin{pmatrix}c_n\\ s_n\end{pmatrix}\hat{\mathbf{r}} + v\begin{pmatrix}-s_n\\ c_n\end{pmatrix}\hat{\mathbf{t}} + w\begin{pmatrix}c_n\\ s_n\end{pmatrix}\bar{\mathbf{k}} \tag{8}$$

in which $c_n = \cos n\theta$ and $s_n = \sin n\theta$, then the gradient $\nabla\bar{\mathbf{g}}$ can be shown to be given by

$$\begin{aligned}\nabla\bar{\mathbf{g}} = {} & \hat{\mathbf{r}}\left[\frac{\partial u}{\partial r}\begin{pmatrix}c_n\\ s_n\end{pmatrix}\hat{\mathbf{r}} + \frac{\partial v}{\partial r}\begin{pmatrix}-s_n\\ c_n\end{pmatrix}\hat{\mathbf{t}} + \frac{\partial w}{\partial r}\begin{pmatrix}c_n\\ s_n\end{pmatrix}\bar{\mathbf{k}}\right]\\ & + \hat{\mathbf{t}}\left[\frac{nu-v}{r}\begin{pmatrix}-s_n\\ c_n\end{pmatrix}\hat{\mathbf{r}} + \frac{u-nv}{r}\begin{pmatrix}c_n\\ s_n\end{pmatrix}\hat{\mathbf{t}} + \frac{nw}{r}\begin{pmatrix}-s_n\\ c_n\end{pmatrix}\bar{\mathbf{k}}\right]\\ & + \hat{\mathbf{k}}\left[\frac{\partial u}{\partial z}\begin{pmatrix}c_n\\ s_n\end{pmatrix}\hat{\mathbf{r}} + \frac{\partial v}{\partial z}\begin{pmatrix}-s_n\\ c_n\end{pmatrix}\hat{\mathbf{t}} + \frac{\partial w}{\partial z}\begin{pmatrix}c_n\\ s_n\end{pmatrix}\bar{\mathbf{k}}\right]\end{aligned} \tag{9}$$

In this expression, the products $\hat{\mathbf{r}}\hat{\mathbf{r}}$, $\hat{\mathbf{r}}\hat{\mathbf{t}}$, etc. must be interpreted as dyads.

Figure 2 shows the nine simple dipoles, chosen so that the forces in the first octant are always pointing in the positive direction; the directions of the dipoles are then defined by the right-hand rule. Applying eqn (9) to the Green's functions for horizontal and vertical loads given by eqns (1) and (3) and deciding on the appropriate unit direction $\hat{\mathbf{a}}$ from Fig. 2 (where it coincides with one of the Cartesian base vectors $\hat{\mathbf{i}}$, $\hat{\mathbf{j}}$, $\hat{\mathbf{k}}$, namely $\hat{\mathbf{i}} = \hat{\mathbf{r}}\cos\theta - \hat{\mathbf{t}}\sin\theta$, $\hat{\mathbf{j}} = \mathbf{r}\sin\theta + \hat{\mathbf{t}}\cos\theta$, or $\hat{\mathbf{k}} = \hat{\mathbf{k}}$), one obtains after some algebra the displacements for both crack sources (M_{xx}, M_{yy}, M_{zz}) and for single couples (M_{xy}, M_{xz}, etc.). The results are summarized in Table 1. The Green's functions for dipoles are constructed from this table multiplying the coefficients in a given column by the expressions in the first column and adding the result. For example, the Green's function for a crack M_{xx} is

$$\begin{aligned}\bar{\mathbf{u}} = -\frac{M_{xx}}{2}\Bigg\{ & \left(\frac{\partial u}{\partial r} + \frac{u-v}{r}\right)\hat{\mathbf{r}} + \left(\frac{\partial w}{\partial r} + \frac{w}{r}\right)\hat{\mathbf{k}}\\ & + \left(\frac{\partial u}{\partial r} - \frac{u-v}{r}\right)\cos 2\theta\hat{\mathbf{r}} - \left(\frac{\partial v}{\partial r} + \frac{u-v}{r}\right)\sin 2\theta\hat{\mathbf{t}} + \left(\frac{\partial w}{\partial r} - \frac{w}{r}\right)\cos 2\theta\hat{\mathbf{k}}\Bigg\}\end{aligned} \tag{10}$$

Evaluation of the equations derived from Table 1 by means of the Thin Layer Method requires appropriate expressions for the derivatives with respect to r and z for the terms in the first column. These are obtained from eqns (2) and (4); the final results are:

$$\frac{\partial u}{\partial r} + \frac{u-v}{r} = \frac{1}{r}\left(\frac{\partial(ru)}{\partial r} - v\right) = -\frac{1}{4i}\sum_{l=1}^{2N}\phi_x^l(z)\phi_x^l(z')k_l H_1^{(2)}(k_l r) \tag{11a}$$

$$\frac{\partial v}{\partial r} - \frac{u-v}{r} = \frac{1}{r}\left(\frac{\partial(rv)}{\partial r} - u\right) = -\frac{1}{4i}\sum_{l=1}^{N}\phi_y^l(z)\phi_y^l(z')k_l H_1^{(2)}(k_l r) \tag{11b}$$

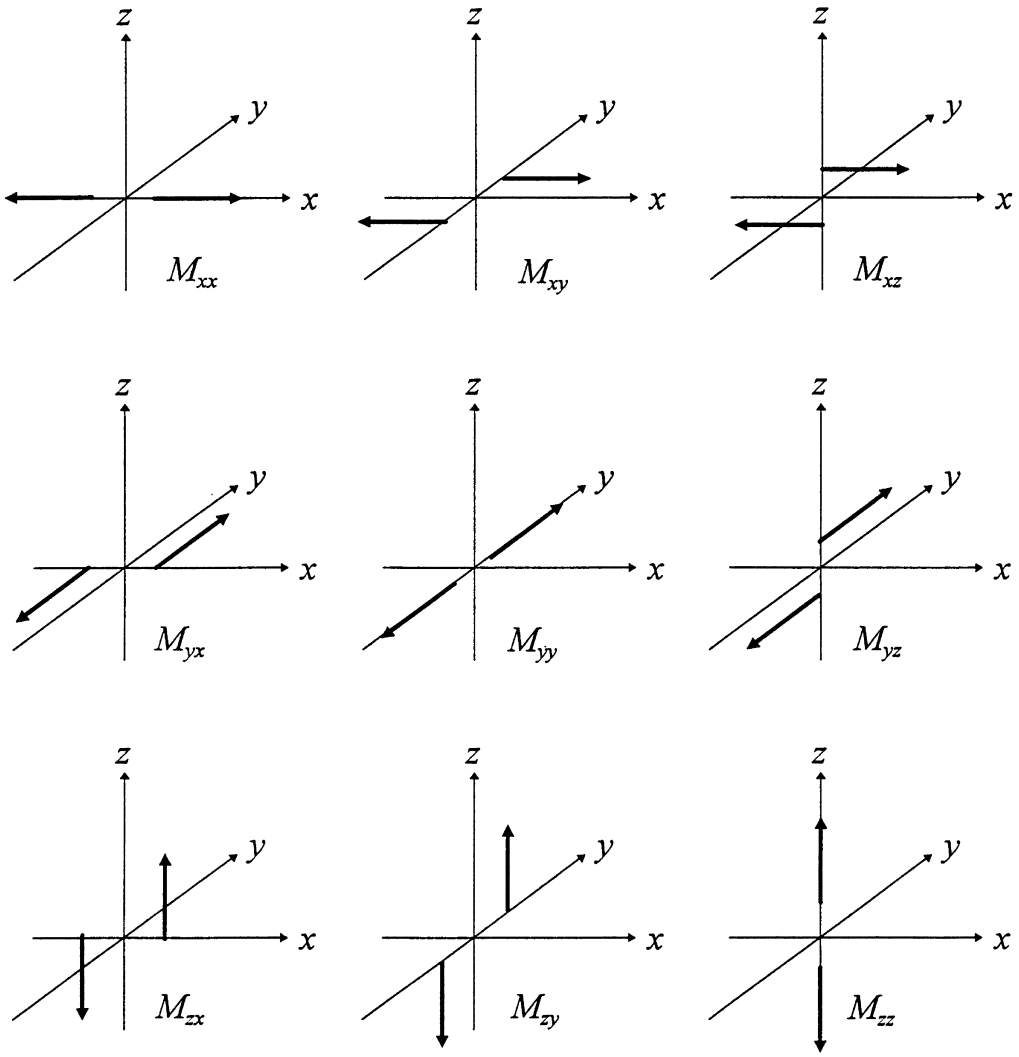

Fig. 2. The nine force dipoles.

$$\frac{\partial w}{\partial r}+\frac{w}{r}=-\frac{1}{4i}\sum_{l=1}^{N}\phi_z^l(z)\phi_x^l(z')k_l H_0^{(2)}(k_l r) \tag{11c}$$

$$\frac{\partial u}{\partial r}-\frac{u-v}{r}=\left(\frac{\partial u}{\partial r}+\frac{u-v}{r}\right)-2\frac{u-v}{r} \quad \text{[apply (11a) and (2a,b)]} \tag{11d}$$

$$\frac{\partial v}{\partial r}+\frac{u-v}{r}=\left(\frac{\partial v}{\partial r}-\frac{u-v}{r}\right)+2\frac{u-v}{r} \quad \text{[apply (11b) and (2a,b)]} \tag{11e}$$

Table 1
Coefficients for simple dipoles (cracks and single couples) $c_n = \cos n\theta$, $s_n = \sin n\theta$

	$-\frac{1}{2}M_{xx}$	$-\frac{1}{2}M_{xy}$	$-M_{xz}$	$-\frac{1}{2}M_{yx}$	$-\frac{1}{2}M_{yy}$	$-M_{yz}$	$-M_{zx}$	$-M_{zy}$	$-M_{zz}$
$\left(\frac{\partial u}{\partial r}+\frac{u-v}{r}\right)\hat{\mathbf{r}}$	1				1				
$\left(\frac{\partial v}{\partial r}-\frac{u-v}{r}\right)\hat{\mathbf{t}}$		-1		1					
$\left(\frac{\partial w}{\partial r}+\frac{w}{r}\right)\hat{\mathbf{k}}$	1				1				
$\left(\frac{\partial u}{\partial r}-\frac{u-v}{r}\right)\hat{\mathbf{r}}$	c_2	s_2		s_2	$-c_2$				
$\left(\frac{\partial v}{\partial r}+\frac{u-v}{r}\right)\hat{\mathbf{t}}$	$-s_2$	c_2		c_2	s_2				
$\left(\frac{\partial w}{\partial r}-\frac{w}{r}\right)\hat{\mathbf{k}}$	c_2	s_2		s_2	$-c_2$				
$\frac{\partial u}{\partial z}\hat{\mathbf{r}}$			c_1			s_1			
$\frac{\partial v}{\partial z}\hat{\mathbf{t}}$			$-s_1$			c_1			
$\frac{\partial w}{\partial z}\hat{\mathbf{k}}$			c_1			s_1			
$\frac{\partial U}{\partial r}\hat{\mathbf{r}}$							c_1	s_1	
$\frac{U}{r}\hat{\mathbf{t}}$							$-s_1$	c_1	
$\frac{\partial W}{\partial r}\hat{\mathbf{k}}$							c_1	s_1	
$\frac{\partial U}{\partial z}\hat{\mathbf{r}}$									1
$\frac{\partial W}{\partial z}\hat{\mathbf{k}}$									1

$$\frac{\partial w}{\partial r}-\frac{w}{r}=\left(\frac{\partial w}{\partial r}+\frac{w}{r}\right)-2\frac{w}{r} \quad \text{[apply (11c) and(2c)]} \tag{11f}$$

$$\frac{\partial U}{\partial r}=-\frac{U}{r}+\frac{1}{4i}\sum_{l=1}^{2N}\phi_x^l(z)\phi_z^l(z')k_lH_0^{(2)}(k_lr) \tag{11g}$$

$$\frac{\partial W}{\partial r}=-\frac{1}{4i}\sum_{l=1}^{2N}\phi_z^l(z)\phi_z^l(z')k_lH_1^{(2)}(k_lr) \tag{11h}$$

As for the vertical derivatives, they are obtained from eqns (2a–c) substituting in the summations the first factors, $\phi_x^l(z)$, $\phi_y^l(z)$, $\phi_z^l(z)$ with their corresponding partial derivatives. Since the medium has been discretized in the vertical direction, these derivatives must be obtained by consideration of the interpolation polynomials $\mathbf{N}(z)$ on which the formulation is based. When using a linear expansion, these derivatives are discontinuous across the layer interfaces, in which case it is best to evaluate the Green's functions only at the center of the layers. On the other hand, if quadratic (or higher) expansion is used, the Green's functions remain continuous across the layer interfaces.

Denote with z_t, z_b the elevations of the top and bottom interfaces, respectively, of the thin layer containing z, so that $h=z_t-z_b$ is the thickness of that layer. Let $\zeta=(z-z_b)/h$ be the dimensionless vertical coordinate. The isoparametric interpolation polynomials, their derivatives and the modal values are then as follows:

(a) Linear expansion

$$\mathbf{N}=[\zeta \quad (1-\zeta)] \tag{12a}$$

$$\frac{\partial}{\partial z}\mathbf{N}=\frac{1}{h}[1 \quad -1] \tag{12b}$$

$$\phi_x^l(z)=\mathbf{N}\begin{Bmatrix}\phi_x^{tl}\\ \phi_x^{bl}\end{Bmatrix} \tag{12c}$$

$$\frac{\partial\phi_x^l(z)}{\partial z}=\frac{\phi_x^{tl}-\phi_x^{bl}}{h} \tag{12d}$$

in which $\phi_x^{tl}=\phi_x^l(z_t)$ and $\phi_x^{bl}=\phi_x^l(z_b)$ are the values of ϕ_x^l at the top and bottom interfaces, respectively, of the layer which contains the observation point at depth z. Similar expressions can be written for $\phi_y^l(z)$, $\phi_z^l(z)$ and their derivatives.

(b) Quadratic expansion

$$\mathbf{N}=[2\zeta^2-\zeta \quad 4\zeta-4\zeta^2 \quad 1-3\zeta+2\zeta^2] \tag{13a}$$

$$\frac{\partial}{\partial z}\mathbf{N}=\frac{1}{h}[4\zeta-1 \quad 4-8\zeta \quad 4\zeta-3] \tag{13b}$$

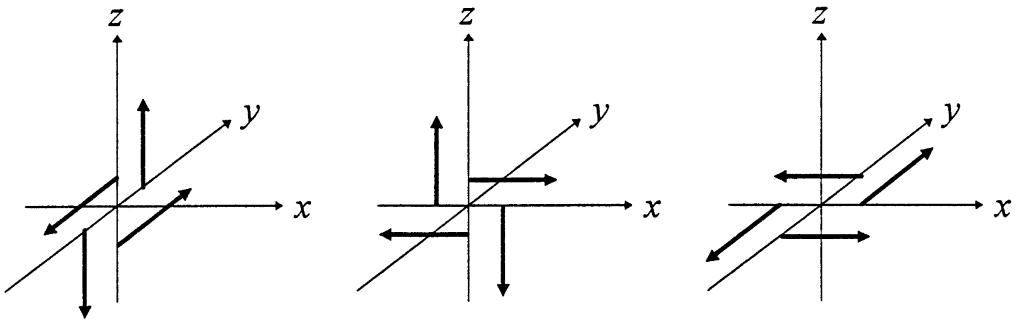

Fig. 3. Pure moments.

$$\phi_x^l(z) = \mathbf{N}\begin{Bmatrix}\phi_x^{tl}\\ \phi_x^{ml}\\ \phi_x^{bl}\end{Bmatrix} \tag{13c}$$

in which ϕ_x^{ml} refers to the intermediate nodal interface.

As an example of the above, the derivative of U [eqn (4a)] with respect to z when using a linear expansion, is given by

$$\frac{\partial U}{\partial z} = \frac{1}{4i}\sum_{l=1}^{2N}\frac{\phi_x^{tl}-\phi_x^{bl}}{h}\phi_z^l(z')H_1^{(2)}(k_l r) \tag{14}$$

Similar expressions can be written for all other derivatives of the Green's functions by simple inspection of eqns (2a–c) and (4b). As for the modal values at the elevation of the load [i.e. $\phi_x^l(z')$, etc.], they are again obtained applying eqns (12c) or (13c), but using the modal values that correspond to the layer containing the load.

5. Pure moments (double couples)

The Green functions for pure torsional and rocking moments are obtained combining the Green's functions for two single couples of equal strength (Fig. 3):

$$M_x = M_{zy} - M_{yz} \quad M_y = M_{xz} - M_{zx} \quad M_z = M_{yx} - M_{xy} \tag{15}$$

This results in the following expressions:

(a) Rocking about x:

$$\bar{\mathbf{u}} = \frac{M_x}{2}\left\{\left(\frac{\partial u}{\partial z} - \frac{\partial U}{\partial r}\right)\sin\theta\hat{\mathbf{r}} + \left(\frac{\partial v}{\partial z} - \frac{U}{r}\right)\cos\theta\hat{\mathbf{t}} + \left(\frac{\partial w}{\partial z} - \frac{\partial W}{\partial r}\right)\sin\theta\hat{\mathbf{k}}\right\} \tag{16}$$

in which the terms are obtained from eqns (11).

(b) Rocking about y:

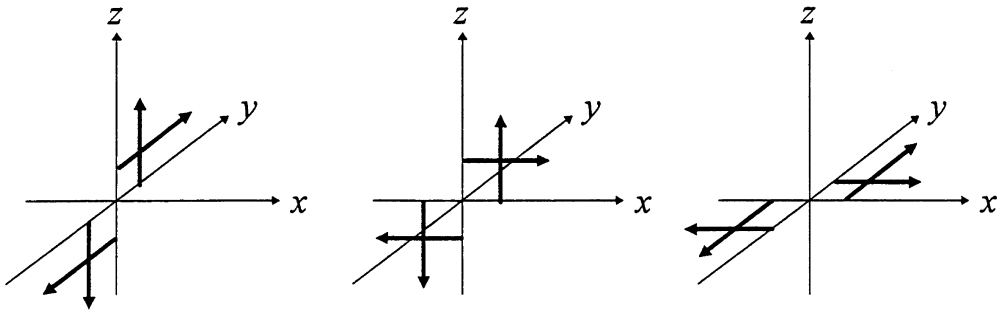

Fig. 4. Seismic moments.

$$\bar{\mathbf{u}} = \frac{M_y}{2}\left\{\left(\frac{\partial U}{\partial r} - \frac{\partial u}{\partial z}\right)\cos\theta\hat{\mathbf{r}} - \left(\frac{U}{r} - \frac{\partial v}{\partial z}\right)\sin\theta\hat{\mathbf{t}} + \left(\frac{\partial W}{\partial r} - \frac{\partial w}{\partial z}\right)\cos\theta\hat{\mathbf{k}}\right\} \tag{17}$$

(c) Torsion about z:

$$\bar{\mathbf{u}} = \frac{M_z}{2}\left(\frac{u-v}{r} - \frac{\partial v}{\partial r}\right)\hat{\mathbf{t}} = \frac{M_z}{2r}\left(u - \frac{\partial(rv)}{\partial r}\right)\hat{\mathbf{t}} \tag{18}$$

6. Double couples (seismic moments) with no net resultant

The three seismic moments are shown in Fig. 4; their Green's functions are obtained by simple addition of the Green's functions for the corresponding single couples. For example, the Green's function for a seismic moment of intensity M_0 ($= M_{xy} = M_{yx}$) and horizontal polarization (i.e. vertical axis) is

$$\bar{\mathbf{u}} = -M_0\left\{\left(\frac{\partial u}{\partial r} - \frac{u-v}{r}\right)\sin 2\theta\hat{\mathbf{r}} + \left(\frac{\partial v}{\partial r} + \frac{u-v}{r}\right)\cos 2\theta\hat{\mathbf{t}} + \left(\frac{\partial w}{\partial r} - \frac{w}{r}\right)\sin 2\theta\hat{\mathbf{k}}\right\} \tag{19}$$

in which the individual terms are again obtained from eqn (11).

7. Bimoments

These are moments of pure moments and have no net resultant. Their Green's functions are obtained in the same fashion as those for single couples, except that the functions for moments are used in place of those for forces. Of the nine possible bimoments, we consider here only the torsional bimoment (Fig. 5),

$$\bar{\mathbf{u}} = -B\left\{\frac{1}{r}\left(\frac{\partial v}{\partial r} - \frac{u-v}{r}\right)\cos\theta\hat{\mathbf{r}} - \frac{\partial}{\partial r}\left(\frac{\partial v}{\partial r} - \frac{u-v}{r}\right)\sin\theta\hat{\mathbf{t}}\right\} \tag{20}$$

which is obtained by substituting into eqn (7) the Green's functions for a torsional moment [eqn

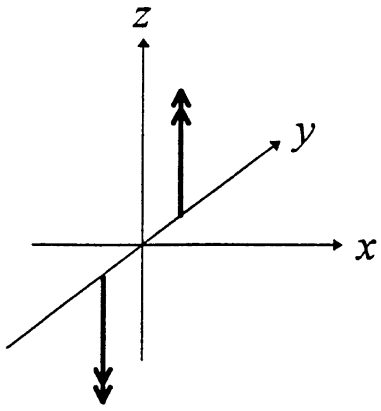

Fig. 5. Bimoment (moment dipole).

(18)] and assuming a strength $B = 2M_z a$. This bimoment is of particular interest here, because together with the Green's functions for a horizontal point load [eqn (2)] and for a rocking point moment [eqn (17)], it constitutes the third independent solution available for a point source producing Green's functions with azimuthal variation $n = 1$ (i.e. with variation $\cos\theta, \sin\theta$); when considered in combination, these three cases find interesting applications in boundary element solutions and in the formulation of transmitting boundaries.

8. Blast loads

To obtain the Green's functions for blast loads, we consider an unbounded, homogeneous elastic solid containing a small spherical cavity of radius a. Within this cavity acts a harmonically oscillating pressure with amplitude p. Hence, the net force acting on an elementary area $\mathrm{d}A$ with position vector $\bar{\mathbf{a}} = a\hat{\mathbf{n}}$ on the cavity's wall (with unit outward normal $\hat{\mathbf{n}}$, see also Fig. 6) is:

$$\begin{aligned} \mathrm{d}\bar{\mathbf{F}} &= p\,\mathrm{d}A\hat{\mathbf{n}} = \mathrm{d}F_x\hat{\mathbf{i}} + \mathrm{d}F_y\hat{\mathbf{j}} + \mathrm{d}F_z\hat{\mathbf{k}} \\ &= p\,\mathrm{d}A(n_x\hat{\mathbf{i}} + n_y\hat{\mathbf{j}} + n_z\hat{\mathbf{k}}) \end{aligned} \tag{21}$$

where $\mathrm{d}F_x$, $\mathrm{d}F_y$, $\mathrm{d}F_z$ are the Cartesian components of the force. Next, consider an external point in the medium with position vector $\bar{\mathbf{r}}$ relative to the center of the cavity; the displacements caused by the elementary forces at that point are

$$\mathrm{d}\bar{\mathbf{u}} = p\,\mathrm{d}A[n_x\bar{\mathbf{g}}_x(\bar{\mathbf{r}} - \bar{\mathbf{a}}) + n_y\bar{\mathbf{g}}_y(\bar{\mathbf{r}} - \bar{\mathbf{a}}) + n_z\bar{\mathbf{g}}_z(\bar{\mathbf{r}} - \bar{\mathbf{a}})] \tag{22}$$

in which $\bar{\mathbf{g}}_x$, $\bar{\mathbf{g}}_y$, $\bar{\mathbf{g}}_z$ are the Green's functions for unit loads in directions x, y, z, respectively, whose argument $\bar{\mathbf{r}} - \bar{\mathbf{a}}$ is the distance from the point of application of the force to the observation point. Expanding these functions in Taylor series, carrying out a straightforward integration over the entire cavity surface, defining a source strength $S = \frac{4}{3}\pi a^3 p$ and considering the limit of an infinitesimal cavity $a \to 0$, one obtains

$$\bar{\mathbf{u}} = -S[\hat{\mathbf{i}} \cdot \nabla\bar{\mathbf{g}}_x + \hat{\mathbf{j}} \cdot \nabla\bar{\mathbf{g}}_y + \hat{\mathbf{k}} \cdot \nabla\bar{\mathbf{g}}_z] \tag{23}$$

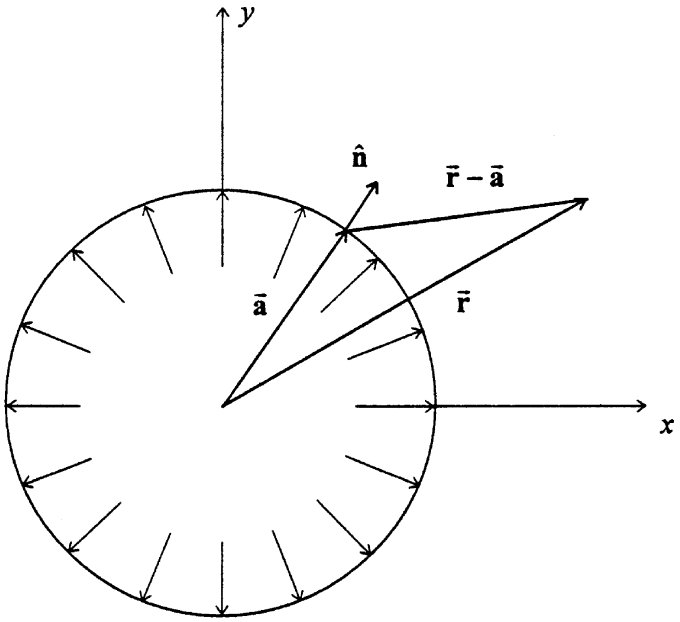

Fig. 6. Blast load.

which provides an initial relationship between the Green's functions for point loads and those for blast loads. As written, however, eqn (23) does not yet provide the correct Green's functions for blast loads, because the functions $\mathbf{g}_x$, $\mathbf{g}_y$, $\mathbf{g}_z$ used in its derivation are those for the continuum and do not consider the presence of the infinitesimally small cavity. A more sophisticated analysis shows that the removal of the tiny particle filling the equally small cavity produces an additional factor in front of eqn (23). When this aspect is taken into account, it can be shown (Kausel, 1998) that the true relationship is

$$\bar{\mathbf{u}} = -\frac{3(\lambda+2\mu)}{4\mu} S[\hat{\mathbf{i}}\cdot\nabla\mathbf{g}_x + \hat{\mathbf{j}}\cdot\nabla\mathbf{g}_y + \hat{\mathbf{k}}\cdot\nabla\mathbf{g}_z] \tag{24}$$

in which λ, μ are the Lamé constants of the layer containing the blast source.

Substituting eqns (2) and (4) into this expression, one obtains after some algebra

$$\mathbf{u} = -\frac{3(\lambda+2\mu)}{4\mu} S\left\{\left(\frac{\partial u}{\partial r} + \frac{u-v}{r} + \frac{\partial U}{\partial z}\right)\hat{\mathbf{r}} + \left(\frac{\partial w}{\partial r} + \frac{w}{r} + \frac{\partial W}{\partial z}\right)\hat{\mathbf{k}}\right\} \tag{25}$$

in which the individual terms are obtained, as before, from eqns (11).

9. Examples of application

We consider in this section a series of numerical benchmark experiments in which we compare numerical results obtained with our program PUNCH, which implements the TLM, with the exact

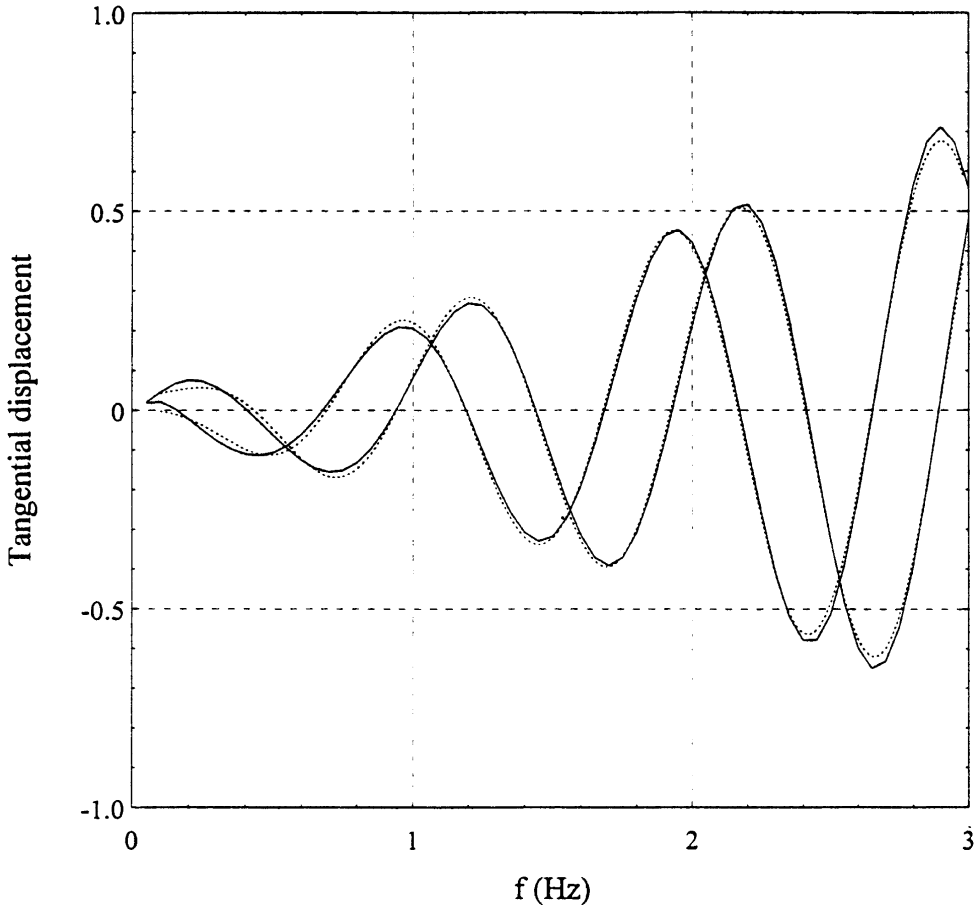

Fig. 7. Torsional point load in an infinite space. Response at $r = 1.0$, $z = 0.2625$.

solutions for those same problems. The purpose of these experiments is to demonstrate the accuracy of the formulas for the TLM presented in this paper and to test the correctness of the program.

As a first example, consider an infinite, homogeneous space subjected to a torsional point load. The exact solution to this problem is

$$v_t(r, z, \omega) = \frac{M_t \cos\varphi}{8\pi\mu R^2}(1 + ib_0)\, e^{-ib_0} \tag{26}$$

in which v_t is the tangential displacement, M_t = torsional moment, $R = \sqrt{r^2 + z^2}$, $\cos\varphi = r/R$, $b_0 = \omega R/\beta$, ω = the frequency (in rad/s), μ = shear modulus and β = shear wave velocity. Figure 7 shows a comparison at one point between the exact solution (solid lines) and the response obtained with the thin layer method (dashed lines), assuming unit material properties and a damping ratio $\zeta = 0.0001$. In the discrete case, the full space was modeled with a homogenous finite layer of unit depth (subdivided into 40 layers of thickness 0.025 each), to which paraxial

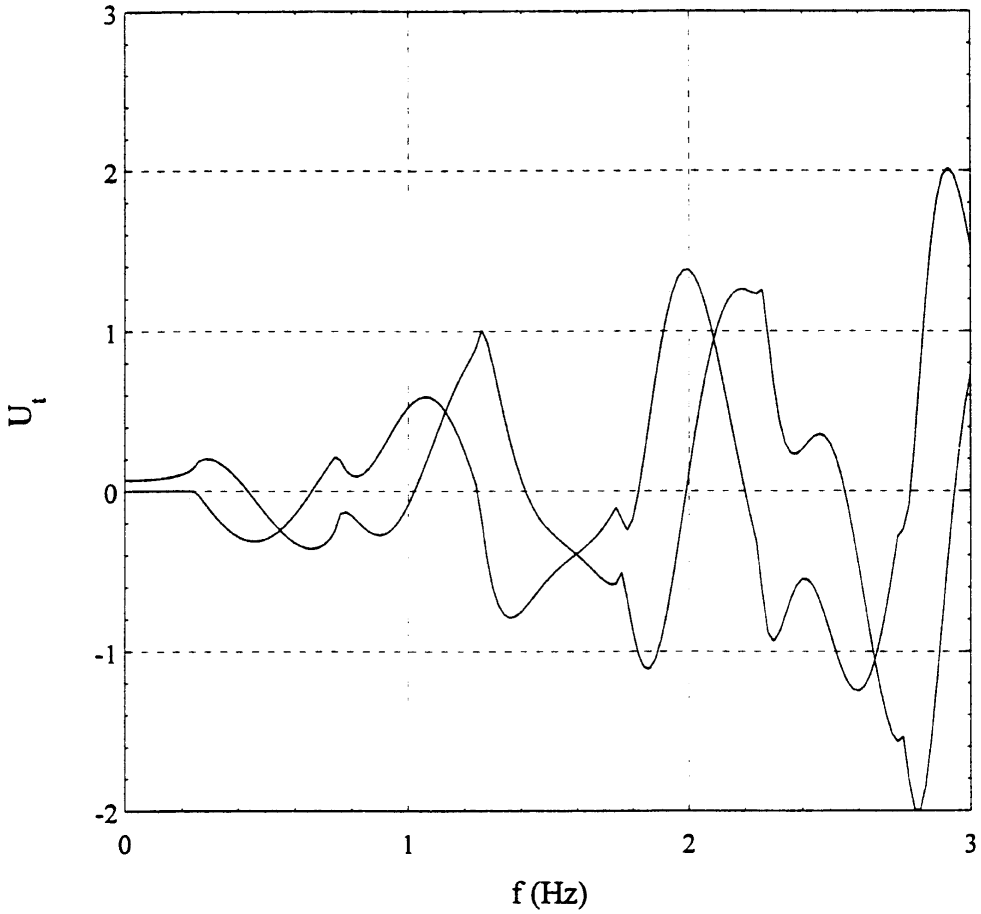

Fig. 8. Torsional point load on the surface of a stratum. Response at $r = 1.0$, $z = 0.0$ (surface).

boundaries were added at the top and bottom interfaces to simulate the infinite medium; the torsional load was placed at the origin in the middle of the 21st sublayer (i.e. 0.0125 units below the geometric center of the model). The output point shown is located halfway between the level of the source and the boundaries, at an epicentral distance equal to the depth of the discrete model. As can be seen, the agreement is nearly perfect. Clearly, the computational effort required for this example using the TLM (less than 2 min for 150 frequencies on a Gateway 120 MHz PC) would have been exactly the same if each of the layers had been made of different materials (including transverse anisotropy), but a benchmark would have been lacking. It is worth pointing out that this example not only demonstrates the correctness of the torsional point load solution implemented in the TLM, but also demonstrates the accuracy of the paraxial boundaries used. Other points at various distances from the source produced equally good results.

Next, we tested the solution for a torsional point load acting at the surface of a homogeneous stratum, using the same model as before but with free and fixed boundaries at the top and bottom,

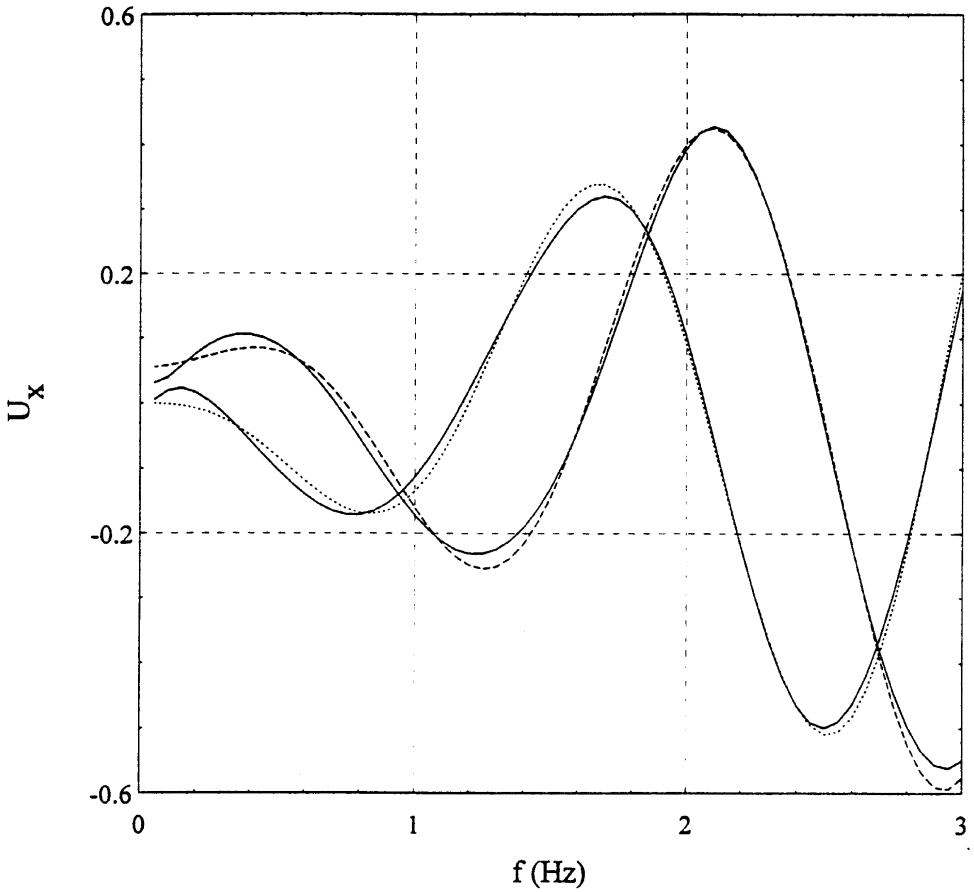

Fig. 9. Blast source in a homogeneous infinite space. Horizontal response at $r = 1.0$, $z = 0.26$.

respectively. Since this problem still involves only SH waves, the exact solution can be derived from eqn (26) by the method of images, which yields

$$v_t(r, z, \omega) = \frac{M_t x}{4\pi\mu} \sum_{j=-\infty}^{\infty} (-1)^j \frac{(1+ib_{0j})\, e^{-ib_{0j}}}{R_j^3} \tag{27}$$

with $z_j = 2hj+z$, $R_j = \sqrt{x^2+z_j^2}$ and $b_{0j} = \omega R_j/\beta$. A comparison between the discrete and exact solutions are shown in Fig. 8; the agreement is so good that differences cannot be resolved at the scale of the plot.

As a third case, we consider a pulsating infinitesimal cavity at the center of an infinite, homogeneous medium, using the same TLM model as for the torsional point load. This problem is interesting because, while the exact solution involves only P (or compressional) waves, the TLM solution includes all wave types (particularly as a result of the paraxial boundaries); remarkably,

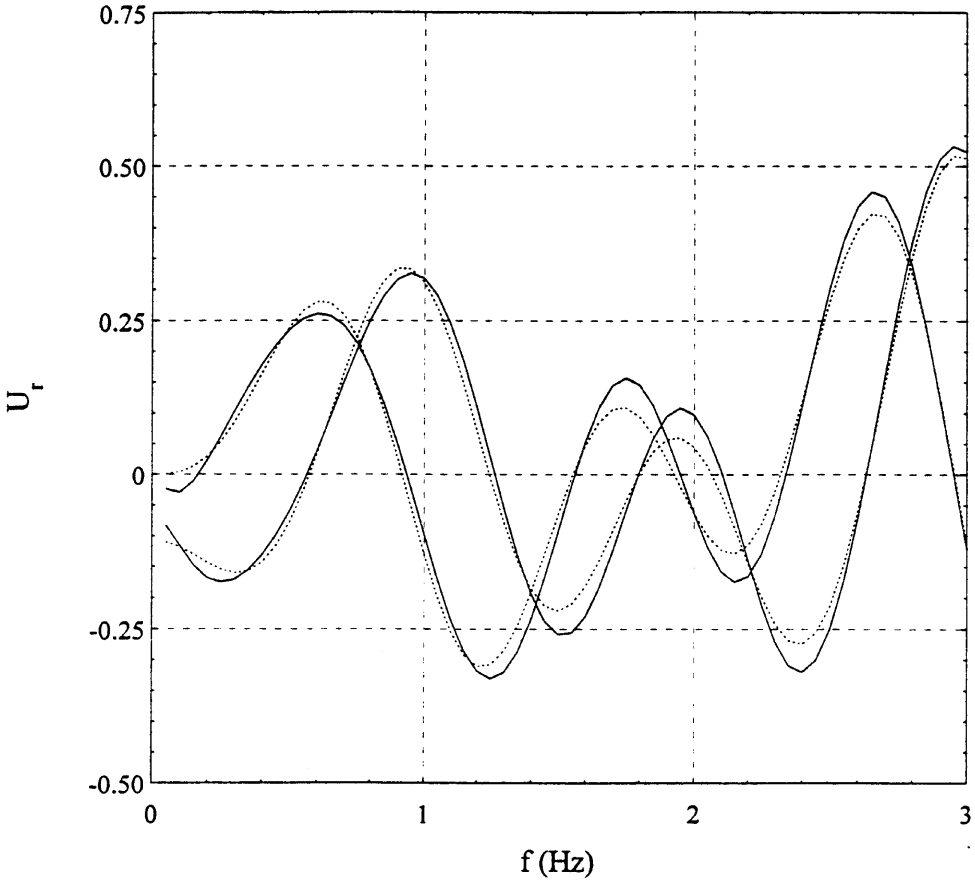

Fig. 10. Horizontally polarized seismic double couple in an infinite space. Radial response at $r = 1.0$, $z = 0.0$, $\theta = 45^\circ$.

the discrete model still produced a decoupled wave field in this case. The exact solution for the radial displacement produced by a pulsating point source (which are spherically symmetric) is

$$u_r = \frac{3S}{16\pi\mu R^2}(1 + ia_0)\,\mathrm{e}^{-ia_0} \tag{28}$$

with S being the source strength, $a_0 = \omega R/\alpha$, α = P-wave velocity, $R = \sqrt{r^2 + z^2}$. Figure 9 shows a comparison of the displacements obtained using the TLM and those of formula (28). Once more, the agreement is excellent and again, the model could have been run with different material properties, without added effort.

As a final example, we consider a horizontally polarized seismic double couple in an infinite, homogeneous space, once more using the paraxial boundaries at the upper and lower surfaces of the model. Instead of using an exact formula for this case, however, we computed the reference solution using the well known Stokes' tensor for a point force, simulating the double couple with four forces appropriately placed in close proximity. Figure 10 shows the results of this exercise and once more the agreement is excellent.

10. Conclusion

In this paper, we presented formulas for the application of the Thin Layer Method (TLM) to the solution of point sources of various types acting within (or on) horizontally layered media. While the formulas presented have general validity and could even be used for laminated media with transverse anisotropy, examples show that they produce accurate results for benchmark problems with known solution. Of course, the main field of application of these formulas is for complex media that are not amenable to analytical treatment, which can be solved by means of the TLM with the same computational effort required for homogeneous media.

References

Bougacha, S., Tassoulas, J.L., 1991. Seismic analysis of gravity dams I: modeling of the sediments. J. Eng. Mech., ASCE 117 (8), 1826–1837.

Bougacha, S., Tassoulas, J.L., Roësset, J.M., 1993. Analysis of foundations on fluid-filled poroelastic stratum. J. Eng. Mech., ASCE 119 (8), 1632–1648.

Dong, S.B., Nelson, R.B., 1972. On natural vibrations and waves in laminated orthotropic plates. J. App. Mech., ASME 39, 739–745.

Dong, S.B., Pauley, K., 1978. Plane waves in anisotropic plates. J. Eng. Mech., ASCE 104 (4), 801–817.

Drake, L.A., 1972. Love and Rayleigh waves in non-horizontally layered media. Bull. Seism. Soc. Am. 62 (5), 1241–1258.Drake, L.A., 1980. Love and Rayleigh waves in irregular soil layer. Bull. Seism. Soc. Am. 70, 571–582.

Geller, R.J., Hatori, T., 1995. DSM synthetic seismograms using analytic trial functions: plane layered, isotropic, case. Geophys. J. Int. 120, 163–172.

Geller, R.J., Ohminato, T., 1994. Computation of synthetic seismograms and their partial derivatives for heterogeneous media with arbitrary natural boundary conditions using the Direct Solution Method. Geophys. J. Int. 116, 421–446.

Ghibril, R., 1992. On the partial discretization of coupled plane stratified systems. Ph.D. thesis, Department of Civil Engineering, M.I.T., 1992.

Huang, K.H., Dong, S.B., 1984. Propagating waves and edge vibrations in anisotropic composite cylinders. J. Sound Vib. 96 (3), 363–379.

Hull [Seale], S., Kausel, E., 1984. Dynamic loads in layered halfspaces. Proceedings, Fifth Engineering Mechanics Division Specialty Conference, Vol. I. ASCE, Laramie, Wyoming, 1984, pp. 201–204.

Kausel, E. 1974. Forced vibrations of circular foundations on layered media. MIT Research Report R74-11, Department of Civil Engineering, MIT, Cambridge, MA.

Kausel, E., 1981. An explicit solution for the Green's functions for dynamic loads in layered media. MIT Research Report R81–13, Department of Civil Engineering, MIT, Cambridge, MA.

Kausel, E., 1986. Wave propagation in anisotropic layered media. Int. J. Num. Meth. Eng. 23, 1567–1578.

Kausel, E., 1993. Discrete Green's functions for layered media: time domain solution. Proceedings of the NSF workshop "Geophysical Techniques For Site and Material Characterization", 11–12 June 1993, Atlanta, Georgia.

Kausel, E., 1994. Thin-layer method: formulation in the time domain. Int. J. Num. Meth. Eng. 37, 927–941.

Kausel, E., 1998. Blast loads vs. point loads: the missing factor. J. Eng. Mech., ASCE 124 (2), 243–244.

Kausel, E., Peek, R., 1982a. Dynamic loads in the interior of a layered stratum: an explicit solution. Bull. Seism. Soc. Am. 72 (5), 1459–1481 (see also Errata, BSSA, 74, 1984, p. 1508).

Kausel, E., Peek, R., 1982b. Boundary integral method for stratified soils. MIT Research Report R82-50, Department of Civil Engineering, MIT, Cambridge, MA.

Kausel, E., Roësset, J.M., 1975. Dynamic stiffness of circular foundations. J. Eng. Mech., ASCE 101 (6), 771–785.

Kausel, E., Roësset, J.M., 1977. Semi-analytic hyperelement for layered strata. J. Eng. Mech., ASCE 103 (4), 569–588.

Kausel, E., Roësset, J.M., 1981. Stiffness matrices for layered soils. Bull. Seism. Soc. Am. 71 (6), 1743–1761.

Kausel, E., Roësset, J.M., Waas, G., 1975. Dynamic analysis of footings on layered media. J. Eng. Mech., ASCE 101 (5), 679–693.
Kausel, E., Seale, S.H., 1987. Static loads in layered halfspaces. J. App. Mech., ASME 54 (2), pp. 403–408.
Lin, H., Tassoulas, J.L., 1987. Discrete Green's functions for layered strata. Int. J. Num. Meth. Eng. 24, 1645–1658.
Lofti, V., Roësset, J.M., Tassoulas, J.L., 1987. A technique for the analysis of the response of dams to earthquakes. Earthq. Eng. Struct. Dyn. 15, 463–490.
Lysmer, J., 1970. Lumped mass method for Rayleigh waves. Bull. Seism. Soc. Am. 43, 17–34.
Lysmer, J., Waas, G., 1972. Shear waves in plane infinite structures. J. Eng. Mech, ASCE 18, 85–105.
Nelson, R.B., Dong, S.B., 1973. High frequency vibrations and waves in laminated orthotropic plates. J. Sound Vib. 30(1), 33–44.
Nelson, R.B., Dong, S.B., Kalra, R.D., 1971. Vibrations and waves in laminated orthotropic circular cylinders. J. Sound Vib. 18, 429–444.
Rukos, E.A., 1978. Continuous elements in the finite element method. Int. J. Num. Meth. Eng., 12, 11–33.
Seale, S.H., 1985. Dynamic loads in layered halfspaces. Ph.D. thesis, Department of Civil Engineering, M.I.T., Cambridge, MA.
Seale, S.H., Kausel, E., 1989. Point loads in cross-anisotropic, layered halfspaces. J. Eng. Mech., ASCE 115 (3), 509–524.
Seale, S.H., Kausel, E., 1990. Dynamic and static impedances of cross-anisotropic halfspaces. Soil Dyn, Earthq. Eng. 9, 4.
Srinivas, S., 1973. A refined analysis of composite laminates. J. Sound Vib. 30 (4), 495–507.
Tajimi, H., 1980. A contribution to theoretical prediction of dynamic stiffness of surface foundations. Proc. 7th W. Conf. Earthq. Eng., Vol. 5. Istanbul, Turkey, 5, pp. 105–112.
Tan, H.H., 1989. Displacement approach for generalized Rayleigh waves in layered solid–fluid media. Bull. Seism. Soc. Am. 79 (4), 1251–1263.
Tassoulas, J., 1981. Elements for the numerical analysis of wave motion in layered media. MIT Research Report R81-2, Department of Civil Engineering, Cambridge, MA.
Tassoulas, J.L., Kausel, E., 1983. Elements for the numerical analysis of wave motion in layered strata. Int. J. Num. Meth. Eng. 19, 1005–1032.
Tassoulas, J.L., Kausel, E., 1983. On the dynamic stiffness of circular ring footings on an elastic stratum. Int. J. Num. Anal. Meth. Geomech. 8, 411–426.
Tsai, C., Lee, G.C., Ketter, R.L., 1990. A semi-analytical method for time-domain analyses of dam–reservoir interactions. Int. J. Num. Eng. 29, 913–933.
Waas, G., 1972. Linear two-dimensional analysis of soil dynamic problems in semi-infinite layer media. Ph.D. thesis, University of California, Berkeley.
Waas, G., 1980. Dynamisch belastete Fundamente auf geschichtetem Baugrund. VDI Berichte 381, 185–189 (in German).
Zinn, R., 1988. Wave propagation in anisotropic laminated rods. M.Sc. thesis, Department of Civil Engineering, M.I.T., Cambridge, MA.